Inorg. Chem. **2007**, *46*, 9548–9557

Inorganic Chemistry Article

Isolation of a Pentadentate Ligand and Stepwise Synthesis, Structures, and Magnetic Properties of a New Family of Homo- and Heterotrinuclear Complexes

Ling-Ling Zheng, Wei-Xiong Zhang, Lian-Jing Qin, Ji-Dong Leng, Jun-Xian Lu, and Ming-Liang Tong*

MOE Key Laboratory of Bioinorganic and Synthetic Chemistry, State Key Laboratory of Optoelectronic Materials and Technologies, School of Chemistry and Chemical Engineering, Sun Yat-Sen University, Guangzhou 510275, P. R. China

Received February 22, 2007

A neutral pentadentate ligand, di(pyrazolecarbimido)amine (Hdcadpz), and its adduct with $HClO_4$, $[H_2dcadpz]^+[ClO_4]^-$, were for the first time isolated from our previously reported $[Cu_3(dcadpz)_2(Hpz)_2(ClO_4)_2](ClO_4)_2{\cdot}H_2O$ by the use of $(NH_4)_2S$ to remove the Cu^{II} ions and characterized by IR, EA, UV, NMR, MS, and X-ray crystallography. Reactions of copper(II) or nickel(II) nitrate with Hdcadpz in a 1:2 molar ratio generated two mononuclear precursors of $[Cu(dcadpz)_2]$ (**1**) and $[Ni(dcadpz)_2]{\cdot}2/3DMF$ (**2**). Furthermore, three new linear homo- and heterotrinuclear complexes of the same motif $[M\{M'(dcadpz)_2\}M]$ ($M = Co^{II}, Ni^{II}$, $M' = Cu^{II}, Ni^{II}$), $[\{Co(pdm)\}_2\{Cu(dcadpz)_2\}](NO_3)_4$ (**3**), $[\{Ni(pdm)\}_2\{Cu(dcadpz)_2\}](NO_3)_4$ (**4**), and $[\{Ni(MeOH)(H_2O)_2\}_2\{Ni(dcadpz)_2\}](NO_3)_4$ (**5**), were synthesized from these two precursors (pdm = 2,6-pyridinedimethanol) and characterized by X-ray crystallography. Magnetic studies show that the central $Cu(dcadpz)_2$ motif is antiferromagnetically coupled with both the terminal Co(II) atoms via the $dcadpz^-$ ligand in **3** with a J value of $-5.27\ cm^{-1}$ and ferromagnetically coupled with both the terminal Ni(II) atoms in **4** with a J value of $2.50\ cm^{-1}$, while **5** behaves only as a Curie paramagnet between 2 and 300 K due to the diamagnetic character of the central square-planar Ni(II) atom.

Introduction

Polynuclear complexes or metal cluster compounds with highly ordered solid-state structures and high-spin ground states have attracted much attention in the past decades.[1,2] In homometallic systems, ferromagnetic and antiferromagnetic behaviors can both occur depending on the bridging modes, bridging angles, and other factors.[3] Although some typical examples with high-spin ground states along with ferromagnetic behavior have been achieved by applying the concept of strict orthogonality[4] between two magnetic orbitals in designing molecules, rational design and synthesis of novel metal clusters with large ground spin states is still a challenging and central topic in the field of molecular magnetism. Development of new metalloligands,[2a,5] which has been found to takes roles not only in mediating magnetic interaction but also in catalytic sites in metal cluster compounds, is undoubtedly one of best ways to meet this challenge. In a recent communication,[6a] we described attempts to synthesize coordination polymers with metal(II) salts and sodium dicyanamide (Na(dca)).[7] An unexpected functional pentadentate ligand, di(pyrazolecarbimido)aminate ($dcadpz^-$), was generated via a simultaneous addition reaction of dicyanamide and pyrazole, which led to in-situ synthesis of a ferromagnetic homotrinuclear copper(II) cluster, from

* To whom correspondence should be addressed. E-mail: tongml@mail.sysu.edu.cn.

(1) (a) Kahn, O. *Molecular Magnetism*; VCH Publishers: Weinheim, 1993. (b) Miller, J. S.; Drillon, M., Eds. *Magnetism: Molecules to Materials II: Molecule-Based Materials*; WILEY-VCH Verlag GmbH: Weinheim, 2001.
(2) (a) Kahn, O. *Acc. Chem. Res.* **2000**, *33*, 647. (b) Thompson, L. K. *Coord. Chem. Revs.* **2002**, *233–234*, 193. (c) Escuer, A.; Aromí, G. *Eur. J. Inorg. Chem.* **2006**, 4721.
(3) Rodríguez-Martín, Y.; Hernández-Molina, M.; Delgado, F. S.; Pasán, J.; Ruiz-Pérez, C.; Sanchiz, J.; Lloret, F.; Julve, M. *CrystEngComm* **2002**, *4*, 522.
(4) Kahn, O.; Galy, J.; Journaux, Y.; Jaid, J.; Morgenstern-Badarau, I. *J. Am. Chem. Soc.* **1982**, *104*, 2165.
(5) (a) Noro, S.-i.; Kitagawa, S.; Yamashita, M.; Wada, T. *Chem. Commun.* **2002**, 222. (b) Noro, S.-i.; Miyasaka, H.; Kitagawa, S.; Wada, T.; Okubo, T.; Yamashita, M.; Mitani, T. *Inorg. Chem.* **2005**, *44*, 133.
(6) (a) Tong, M.-L.; Wu, Y.-M.; Tong, Y.-X.; Chen, X.-M.; Chang, H.-C.; Kitagawa, S. *Eur. J. Inorg. Chem.* **2003**, 2385. (b) Igashira-Kamiyama, A.; Kajiwara, T.; Konno, T.; Ito, T. *Inorg. Chem.* **2006**, *45*, 6460.
(7) Tong, M.-L.; Ru, J.; Wu, Y.-M.; Chen, X.-M.; Chang, H.-C.; Mochizuki, K.; Kitagawa, S. *New J. Chem.* **2003**, *27*, 779.

10.1021/ic070343z CCC: $37.00

Published on Web 10/04/2007

which an interesting metalloligand [Cu(dcadpz)$_2$] was isolated.[6a] As an extension of our continuing interest in such systems, herein we report isolation and characterization of the free pentadentate ligand and the use of such ligand to rationally assemble a new family of magnetic linear homo- and heterotrinuclear metal complexes. They are mononuclear precursors [Cu(dcadpz)$_2$] (**1**) and [Ni(dcadpz)$_2$]·2/3DMF (**2**) and linear homo- and heterotrinuclear complexes [{Co(pdm)}$_2${Cu(dcadpz)$_2$}](NO$_3$)$_4$ (**3**), [{Ni(pdm)}$_2${Cu(dcadpz)$_2$}](NO$_3$)$_4$ (**4**) (pdm = 2,6-pyridinedimethanol), and [{Ni(MeOH)(H$_2$O)$_2$}$_2${Ni(dcadpz)$_2$}](NO$_3$)$_4$ (**5**).

Experimental

Materials and Physical Measurements. [Cu$_3$(dcadpz)$_2$(Hpz)$_2$(ClO$_4$)$_2$](ClO$_4$)$_2$·H$_2$O was synthesized according to the reported method.[6a] Other reagents and solvents employed were commercially available and used as received without further purification. The C, H, and N microanalyses were carried out with an Elementar Vario-EL CHNS elemental analyzer. ^{1}H and ^{13}C NMR spectra were obtained on a Mercury-Plus 300 spectrometer, and (CD$_3$)$_2$SO was used as solvent. The MS spectra were recorded on Japanese LCMS-2010A mass spectrometer. The FT-IR spectra were recorded from KBr pellets in the range 4000−400 cm^{-1} on a Bio-Rad FTS-7 spectrometer. The UV−vis spectra (Figure S1) were measured on UV−vis−NIR spectrophotometer (UV-3150). Variable-temperature magnetic susceptibility measurements were made using a SQUID magnetometer MPMS XL-7 (Quantum Design) at 0.1 T for **3**, **4**, and **5**. The diamagnetic correction for each sample was determined from Pascal's constants.

Synthesis of Hdcadpz. The crushed single-crystalline powder sample of [Cu$_3$(dcadpz)$_2$(Hpz)$_2$(ClO$_4$)$_2$](ClO$_4$)$_2$·H$_2$O[6a] (1.147 g, 10 mmol) was mixed with a 100 mL solution of (NH$_4$)$_2$S (0.4 mol dm^{-3}) in 20 mL of H$_2$O and 50 mL of CHCl$_3$ and then was vigorously stirred for 3 h at room temperature. The colorless organic layer was separated and evaporated to dryness. Colorless block crystals of Hdcadpz were obtained by recrystallization from EtOH (yield: ca. 60%). ESI-MS: m/z = 250; ^{1}H NMR (300 MHz, (CD$_3$)$_2$SO): δ 10.42 (1H, N1−H1N), 8.77 (d, J = 2.1 Hz, 4H, C8−H8, C3−H3), 7.85 (d, J = 0.9 Hz, 2H, C6−H6, C1−H1), 6.56 (m, 2H, C2−H2, C7−H7), 9.08 (2H, N3−H3B, N3−H3A); ^{13}C NMR (75 MHz, (CD$_3$)$_2$SO): δ 153.2 (C-3), 129.1 (C-2), 142.8 (C-1), 108.3 (C-4). Anal. Calcd (%) for C$_{16}$H$_{18}$N$_{14}$: C, 47.29; H, 4.46; N, 48.25. Found: C, 47.18; H, 4.65; N,48.17. IR (KBr, cm^{-1}): ν = 3438, 3303 (N−H); 1662 (C=N). UV−vis(H$_2$O): $\lambda_{max,nm}$ = 253.

Synthesis of [H$_2$dcadpz]$^+$[ClO$_4$]$^-$. To the ethanol solution (10 mL) of Hdcadpz (0.020 g, 0.1 mmol) was added a dilute (0.5 M) HClO$_4$ solution (2 mL). Colorless block crystals were formed by slow evaporation at room temperature in 2−3 days. Anal. Calcd (%) for C$_8$H$_{10}$ClN$_7$O$_4$: C, 31.64; H, 3.32; N, 32.29. Found: C, 31.51; H, 3.40; N,32.18. IR (KBr, cm^{-1}): ν = 3315 (N−H); 1665 (C=N); 1470, 1402, 1380 (ClO$_4^-$). UV−vis(H$_2$O): $\lambda_{max,nm}$ = 253.

Synthesis of [Cu(dcadpz)$_2$] (1). Two methods can be used.

Method A. A solution of Hdcadpz (0.041 g, 0.2 mmol) in CH$_3$CN (2 mL) was added to a solution of Cu(NO$_3$)$_2$·3H$_2$O (0.024 g, 0.1 mmol) in EtOH (10 mL). Purple block crystals were formed from the resulting solution by slow evaporation at room temperature, which were collected and dried in air (yield ca. 35%). Anal. Calcd (%) for CuC$_{16}$H$_{16}$N$_{14}$: C, 41.07; H, 3.45; N, 41.91. Found: C, 40.96; H, 3.56; N, 41.86. IR (KBr, cm^{-1}): ν = 3439 (N−H); 1662, 1622 (C=N). UV−vis(CHCl$_3$): $\lambda_{max,nm}$ = 253, 496.

Method B. [Cu$_3$(dcadpz)$_2$(Hpz)$_2$(ClO$_4$)$_2$](ClO$_4$)$_2$·H$_2$O[6a] (0.574 g, 5 mmol) and Na$_2$H$_2$edta (15 mmol) were vigorously stirred for 2 h in a H$_2$O (20 mL)/CHCl$_3$ (20 mL) mixture at room temperature. The purple organic layer was separated and evaporated to dryness. Purple block crystals of **1** were obtained by recrystallization from CHCl$_3$ (yield, 75%).

Synthesis of [Ni(dcadpz)$_2$] 2/3DMF (2). A solution of Hdcadpz (0.041 g, 0.2 mmol) in MeCN (3 mL) was added to a methanol solution (3 mL) of Ni(NO$_3$)$_2$·6H$_2$O (0.029 g, 0.1 mmol). A pink powder was formed 1 week later, and crystals suitable for X-ray diffraction were obtained by dissolving the powder in DMF (2 mL) at room temperature; the crystals were collected and dried in the air (yield ca. 25%). Anal. Calcd for NiC$_{16}$H$_{16}$N$_{14}$: C, 41.50; H, 3.48; N, 42.35. Found: C, 41.38; H, 3.57; N, 42.19. IR (KBr, cm^{-1}): ν = 3451, 3308 (N−H); 1617 (C=N). UV−vis(DMSO): $\lambda_{max,nm}$ = 253, 408, 494.

Synthesis of [{Co(pdm)}$_2${Cu(dcadpz)$_2$}](NO$_3$)$_4$ (3). A methanol solution of Co(NO$_3$)$_2$·6H$_2$O (0.058 g, 0.2 mmol) and pdm (0.020 g, 0.2 mmol) was stirred at room temperature for 30 min, and then a CHCl$_3$ (2 mL) solution of **1** (0.047 g, 0.10 mmol) was added. Deep red crystals were formed from the resulting red solution by slow evaporation at room temperature; the crystals were collected and dried in the air (yield ca. 65%). Anal. Calcd for C$_{30}$H$_{34}$Co$_2$CuN$_{20}$O$_{16}$: C, 32.40; H, 3.08; N, 25.19. Found: C, 32.28; H, 3.16; N, 25.09. IR (KBr, cm^{-1}): ν = 3301 (N−H); 1655 (C=N); 1285 (NO$_3^-$). UV−vis(MeOH): $\lambda_{max,nm}$ = 253, 532.

Synthesis of [{Ni(pdm)}$_2${Cu(dcadpz)$_2$}](NO$_3$)$_4$ (4). Complex **4** was synthesized in an analogous procedure to **3**, except that Co(NO$_3$)$_2$·6H$_2$O was replaced by Ni(NO$_3$)$_2$·6H$_2$O. Pale purple plates of **4** were obtained from the resulting light purple solution by slow evaporation at room temperature; the crystals were collected and dried in the air (ca. 72%). Anal. Calcd for C$_{30}$H$_{34}$Ni$_2$CuN$_{20}$O$_{16}$: C, 32.41; H, 3.08; N, 25.20. Found: C, 32.36; H, 3.17; N, 25.03. IR (KBr, cm^{-1}): ν = 3289 (N−H); 1654 (C=N); 1287 (NO$_3^-$). UV−vis(MeOH): $\lambda_{max,nm}$ = 253, 555, 835.

Synthesis of [{Ni(MeOH)(H$_2$O)$_2$}$_2${Ni(dcadpz)$_2$}](NO$_3$)$_4$ (5). A DMF solution (2 mL) of **2** (0.051 g, 0.067 mmol) was added to a methanol solution (5 mL) of Ni(NO$_3$)$_2$·6H$_2$O (0.058 g, 0.2 mmol). Light purple crystals were obtained from the resulting purple solution by slow evaporation at room temperature; the crystals were collected and dried in the air (yield ca. 42%). Anal. Calcd for C$_{18}$H$_{32}$N$_{18}$Ni$_3$O$_{18}$: C, 22.41; H, 3.34; N, 26.41. Found: C, 22.36; H, 3.64; N, 26.27. IR (KBr, cm^{-1}): ν = 3515, 3303 (N−H); 1652 (C=N); 1308 (NO$_3^-$). UV−vis(MeOH): $\lambda_{max,nm}$ = 255, 430, 506, 842.

X-ray Crystallography. Data collection of Hdcadpz, [H$_2$dcadpz]$^+$[ClO$_4$]$^-$, and **1**−**5** was performed with Mo Kα radiation (λ = 0.71073 Å) on a Bruker Apex CCD diffractometer at 293(2) K or 123(2) K. The intensities were integrated with SAINT$^+$, which also applied corrections for Lorentz and polarization effects. Absorption corrections were applied by using the multiscan program SADABS.[8] The structures were solved by direct methods, and all non-hydrogen atoms were refined anisotropically by least-squares on F^2 using the SHELXTL program.[9] Hydrogen atoms on organic ligands were generated by the riding mode (C−H = 0.93 Å). Crystal data and details of data collection and refinements for Hdcadpz, [H$_2$dcadpz]$^+$[ClO$_4$]$^-$, and complexes **1**−**5** are summarized in Table 1. Selected bond distances and bond angles are listed in Tables 2 and 3.

(8) Sheldrick, G. M. *SADABS 2.05*; University of Göttingen: Göttingen, Germany.
(9) *SHELXTL 6.10*; Bruker Analytical Instrumentation: Madison, WI, 2000.

Table 1. Summary of Crystal Data and Structure Refinements for Hdcadpz, $[H_2dcadpz]^+[ClO_4]^-$ and **1**−**5**

	Hdcadpz	$[H_2dcadpz]^+[ClO_4]^-$	**1**	**2**	**3**	**4**	**5**
formula	$C_{16}H_{18}N_{14}$	$C_8H_{10}ClN_7O_4$	$C_{16}H_{16}CuN_{14}$	$C_{27}H_{31}N_{22}Ni_{1.50}O$	$C_{30}H_{34}Co_2CuN_{20}O_{16}$	$C_{30}H_{34}CuN_{20}Ni_2O_{16}$	$C_{18}H_{32}N_{18}Ni_3O_{18}$
fw	406.44	303.68	467.97	767.80	1112.17	1111.73	964.75
temp (K)	293	293	293	293	123	293	293
cryst syst	triclinic	orthorhombic	tetragonal	monoclinic	triclinic	triclinic	triclinic
space group	$P\bar{1}$	*Pccn*	$P4_2/n$	$P2_1/n$	$P\bar{1}$	$P\bar{1}$	$P\bar{1}$
a (Å)	7.682(2)	5.6286(7)	22.285(8)	11.271(2)	7.4824(6)	7.731(1)	7.959(1)
b (Å)	11.482(3)	13.137(2)	22.285(8)	16.454(2)	8.4117(7)	8.579(1)	9.275(4)
c (Å)	11.716(3)	17.198(2)	3.891(2)	17.633(3)	17.005(1)	16.549(3)	13.231(4)
α (deg)	98.347(5)	90	90	90.00	86.338(2)	85.636(2)	79.18(3)
β (deg)	102.806(4)	90	90	90.632(3)	86.662(2)	84.976(3)	72.88(2)
γ (deg)	100.994(4)	90	90	90.00	68.646(2)	71.365(3)	70.78(2)
vol ($Å^3$)	970.0(4)	1271.7(3)	1932(1)	3270.0(8)	994.1(1)	1034.7(3)	876.9(5)
Z	2	4	4	4	1	1	1
D_{calcd} ($g\ cm^{-3}$)	1.392	1.586	1.609	1.560	1.858	1.784	1.827
μ (mm^{-1})	0.097	0.328	1.169	0.936	1.456	1.507	1.696
R1 [$I > 2\sigma(I)$][a]	0.0545	0.0683	0.0618	0.0592	0.0366	0.0542	0.0366
wR2 [$I > 2\sigma(I)$][b]	0.1487	0.1732	0.0956	0.1182	0.1000	0.1218	0.0806
R1 [all date][a]	0.0672	0.0775	0.1058	0.0999	0.0392	0.0628	0.0671
wR2 [all date][b]	0.1591	0.1805	0.1066	0.1353	0.1023	0.1266	0.0951

[a] $R1 = \sum||F_o| - |F_c||/\sum|F_o|$. [b] $wR2 = [\sum w(F_o^2 - F_c^2)^2/\sum w(F_o^2)^2]^{1/2}$.

Table 2. Selected Bond Lengths (Å) and Angles (deg) for the Hdcadpz and $[H_2dcadpz]^+[ClO_4]^-$ [a]

Hdcadpz			
N(1)−C(4)	1.272(3)	N(2)−C(4)	1.370(3)
N(2)−C(5)	1.309(3)	N(8)−C(12)	1.302(3)
N(3)−C(5)	1.306(3)	N(9)−C(13)	1.375(3)
N(9)−C(12)	1.306(3)	N(10)−C(13)	1.262(3)
N(1)···N(5)	2.790(3)	N(8)···N(5*a*)	2.995(3)
N(1)···N(12*a*)	3.314(3)	N(8)···N(10)	2.648(3)
N(3)···N(14*b*)	2.997(3)	N(10)···N(7*b*)	3.329(3)
N(3)···N(1)	2.644(3)		
N(1)-H(1N)···N(5)	110(2)	N(8)-H(8A)···N(5*a*)	151(2)
N(1)-H(1N)···N(12*a*)	149(2)	N(8)-H(8B)···N(10)	129(2)
N(3)-H(3A)···N(14*b*)	160(2)	N(10)-H(10N)···N(7*b*)	155(2)
N(3)-H(3B)···N(1)	130(2)		
$[H_2dcadpz]^+[ClO_4]^-$			
N(1)−C(1)	1.297(5)	N(2)−C(1)	1.318(4)
N(1)···O(1)	2.95(1)	N(1)···N(4*c*)	3.013(4)
N(1)···O(4*b*)	3.10(1)		
N(1)-H(1A)···O(1)	146(4)	N(1)-H(1B)···N(4*c*)	147(4)
N(1)-H(1A)···O(4*b*)	149(4)		

[a] Symmetry codes for Hdcadpz: *a*) $-x + 2, -y + 2, -z + 1$; *b*) $-x + 1, -y + 2, -z$. Symmetry codes for $[H_2dcadpz]^+[ClO_4]^-$: *b*) $-x + 7/2, -y + 3/2, z$; *c*) $-x + 2, -y + 1, -z + 1$.

Results and Discussion

Synthesis and Characterization. The dicyanamide ligand [dca, $N(CN)_2^-$] has been extensively used during the past few years to generate a wide variety of polymers of different topologies and magnetic properties.[7,10] In our attempt to synthesize coordination polymers with copper(II) salts and sodium dicyanamide [Na(dca)], the Hdcadpz ligand and its linear trinuclear complex of $[Cu_3(dcadpz)_2(Hpz)_2(ClO_4)_2](ClO_4)_2\cdot H_2O$[6a] was, for the first time, synthesized in situ and structurally characterized as the nucleophilic addition product of pyrazole to the cyano groups of dicyanamidate anion in the presence of the Cu^{II} ion (Scheme 1). It should be noted that few examples[11] involving such interesting in-situ nucleophilic addition reaction with dca occurred before our observation, though the metal-mediated and/or metal-catalyzed reactions of RCN species were surveyed in a number of articles including previous reviews on the nitrile reactivity and also certain sections in the recent general reviews on reactivity of RCN ligands.[12] Na_4edta or Na_2H_2-edta is often used as a good chelate reagent to remove metal ions from coordination compounds. As excepted, the two terminal Cu(II) ions can be easily removed by use of Na_2H_2-edta, from which the precursor of **1**[6a] was obtained. Interestingly, **1** was found to crystallize in two polymorphous phases, one was obtained in $CHCl_3$ by us,[6a] another obtained in a mixed EtOH−$CHCl_3$ solution by Igashira-Kamiyama et al.[6b] However, excess H_2edta^{2-} cannot be used to remove the Cu(II) ion from **1**. Recently, Igashira-Kamiyama et al. applied a method similar to our synthetical strategy to synthesized four linear trinuclear complexes of the same motif $[M\{Cu(dcadpz)_2\}M]^{4+}$.[6b] In order to extend and enrich the coordination chemistry of the $dcadpz^-$ ligand, isolation of the free Hdcadpz ligand is therefore needed. We finally found $(NH_4)_2S$ to be an effective precipitation reagent after trying the possible precipitation reagents of LiOH, NaOH, KOH, and R_4NOH (R = Me or Et). More interestingly, the Hdcadpz ligand was observed to have four forms under various conditions. Hdcadpz-A is neutral and observed in solution characterized by the NMR spectra. Hdcadpz-B is also neutral and stable in the solid state, which has been demonstrated by X-ray crystallography. The protonated form of $[H_2dcadpz]^+$ is observed in the solid structure of its adduct with $HClO_4$, $[H_2dcadpz]^+[ClO_4]^-$. The negatively charged $[dcadpz]^-$

(10) Batten, S. R.; Murray, K. S. *Coord. Chem. Rev.* **2003**, *246*, 103.

(11) (a) Cohn, G. *J. Prakt. Chem.* **1911**, *84*, 394. (b) Rembarz, G.; Fischer, E.; Röber, K.-Ch.; Ohff, R.; Crahmer, H. *J. Prakt. Chem.* **1969**, *311*, 889. (c) Rembarz, G.; Brandner, H.; Finger, H. *J. Prakt. Chem.* **1964**, *26*, 314. (d) Kožíšek, J.; Hvastijovč, M.; Kohout, J. *Inorg. Chim. Acta* **1990**, *168*, 157. (e) Boča, R.; Hvastijovč, M.; Kožíše, J.; Valko, M. *Inorg. Chem.* **1996**, *35*, 4794. (f) Bishop, M. M.; Lindoy, L. F.; Mahadev, S.; Turner, P. *J. Chem. Soc., Dalton Trans.* **2000**, 233.

(12) (a) Constable, E. C. *Metals and Ligand Reactivity (New, revised and expanded edition)*; VCH: Weinheim, 2005. (b) Michelin, R. A.; Mozzon, M.; Bertani, R. *Coord. Chem. Rev.* **1996**, *147*, 299. (c) Kukushkin, V. Y.; Pombeiro, A. J. L. *Chem. Rev.* **2002**, *102*, 1771. (d) Burgess, J.; Hubbard, C. D. *Adv. Inorg. Chem.* **2003**, *54*, 71. (e) Kukushkin, V. Y.; Pombeiro, A. J. L. *Inorg. Chim. Acta* **2005**, *358*, 1. (f) Kopylovich, M. N.; Haukka, M.; Kirillov, A. M.; Yu. Kukushkin, V.; Pombeiro, A. J. L. *Chem. Eur. J.* **2007**, *13*, 786. Khripun, A. V.; Yu. Kukushkin, V.; Selivanov, S. I.; Haukka, M.; Pombeiro, A. J. L. *Inorg. Chem.* **2006**, *45*, 5073.

Table 3. Selected Bond Lengths (Å) and Angles (deg) for **1**−**5**

	1		
Cu(1)−N(1)	1.936(3)	Cu(1)−N(3)	1.926(3)
N(3)−Cu(1)−N(1)	87.1(1)	N(3)−Cu(1)−N(1*a*)	92.9(1)
	2		
Ni(1)−N(1)	1.854(3)	Ni(1)−N(3)	1.853(3)
Ni(2)−N(10)	1.852(3)	Ni(2)−N(17)	1.849(3)
Ni(2)−N(8)	1.862(3)	Ni(2)−N(15)	1.873(3)
N(1)⋯N(5)	2.704(5)	N(10)⋯N(14)	2.719(4)
N(3)⋯N(7)	2.737(5)	N(15)⋯O(1)	3.073(4)
N(8)⋯N(12)	2.758(4)	N(17)⋯N(21)	2.722(4)
N(8)⋯O(1)	3.067(4)		
N(3)−Ni(1)−N(1)	89.7(2)	N(3*a*)−Ni(1)−N(1)	90.4(2)
N(10)−Ni(2)−N(17)	89.2(1)	N(10)−Ni(2)−N(8)	89.6(2)
N(17)−Ni(2)−N(8)	178.7(1)	N(10)−Ni(2)−N(15)	178.3(2)
N(17)−Ni(2)−N(15)	89.3(1)	N(8)−Ni(2)−N(15)	91.9(1)
N(1)−H(1N)⋯N(5)	117(3)	N(10)−H(10N)⋯N(14)	114(3)
N(3)−H(3N)⋯N(7)	119(3)	N(15)−H(15N)⋯O(1)	162(3)
N(8)−H(8N)⋯N(12)	118(3)	N(17)−H(17N)⋯N(21)	125(3)
N(8)-H(8N)⋯O(1)	157(3)		
	3		
Cu(1)−N(1)	1.963(3)	Cu(1)−N(3)	1.952(3)
Co(1)−N(2)	2.103(3)	Co(1)−N(4)	2.119(3)
Co(1)−N(8)	2.070(3)	Co(1)−N(6)	2.087(3)
Co(1)−O(1)	2.177(2)	Co(1)−O(2)	2.175(2)
N(3)−Cu(1)−N(1)	88.7(1)	N(3)−Cu(1)−N(1*a*)	91.3(1)
N(8)−Co(1)−N(6)	111.1(1)	N(8)−Co(1)−N(2)	165.2(1)
N(6)−Co(1)−N(2)	75.6(1)	N(8)−Co(1)−N(4)	102.3(1)
N(6)−Co(1)−N(4)	144.3(1)	N(2)−Co(1)−N(4)	75.1(1)
N(8)−Co(1)−O(2)	75.40(9)	N(6)−Co(1)−O(2)	89.21(9)
N(2)−Co(1)−O(2)	91.81(9)	N(4)−Co(1)−O(2)	111.6(1)
N(8)−Co(1)−O(1)	74.76(9)	N(6)−Co(1)−O(1)	85.39(9)
N(2)−Co(1)−O(1)	119.64(9)	N(4)−Co(1)−O(1)	91.73(9)
O(2)−Co(1)−O(1)	145.33(8)		
	4		
Cu(1)−N(1)	1.950(3)	Cu(1)−N(3)	1.962(3)
Ni(1)−N(8)	1.992(3)	Ni(1)−N(2)	2.017(3)
Ni(1)−N(5)	2.049(4)	Ni(1)−N(7)	2.054(4)
Ni(1)−O(2)	2.107(3)	Ni(1)−O(1)	2.134(3)
N(1)−Cu(1)−N(3*a*)	91.0(1)	N(1)−Cu(1)−N(3)	89.0(1)
N(8)−Ni(1)−N(2)	174.9(1)	N(8)−Ni(1)−N(5)	99.6(1)
N(2)−Ni(1)−N(5)	78.6(1)	N(8)−Ni(1)−N(7)	104.2(1)
N(2)−Ni(1)−N(7)	78.0(1)	N(5)−Ni(1)−N(7)	156.1(1)
N(8)−Ni(1)−O(2)	79.1(1)	N(2)−Ni(1)−O(2)	105.7(1)
N(5)−Ni(1)−O(2)	91.1(1)	N(7)−Ni(1)−O(2)	90.9(1)
N(8)−Ni(1)−O(1)	78.9(1)	N(2)−Ni(1)−O(1)	96.5(1)
N(5)−Ni(1)−O(1)	95.3(1)	N(7)−Ni(1)−O(1)	91.8(1)
O(2)−Ni(1)−O(1)	157.8(1)		
	5		
Ni(1)−N(1)	1.883(3)	Ni(1)−N(3)	1.877(3)
Ni(2)−N(2)	2.015(3)	Ni(2)−O(2w)	2.034(3)
Ni(2)−N(5)	2.056(3)	Ni(2)−N(7)	2.058(3)
Ni(2)−O(1)	2.064(3)	Ni(2)-O(1w)	2.094(3)
N(3*a*)−Ni(1)−N(1)	89.1(1)	N(3)−Ni(1)−N(1)	90.9(1)
N(2)−Ni(2)−O(2w)	177.8(1)	N(2)−Ni(2)−N(5)	78.1(1)
O(2w)−Ni(2)−N(5)	102.6(1)	N(2)−Ni(2)-N(7)	78.5(1)
O(2w)−Ni(2)−N(7)	100.8(1)	N(5)−Ni(2)−N(7)	156.6(1)
N(2)−Ni(2)−O(1)	91.7(1)	O(2w)−Ni(2)−O(1)	86.2(1)
N(5)−Ni(2)−O(1)	89.4(1)	N(7)−Ni(2)−O(1)	91.4(1)
N(2)−Ni(2)−O(1w)	92.2(1)	O(2w)−Ni(2)−O(1w)	89.9(1)
N(5)−Ni(2)−O(1w)	89.7(1)	N(7)−Ni(2)−O(1w)	91.2(1)
O(1)−Ni(2)−O(1w)	175.7(1)		

[a] Symmetry code for **1**: *a*) −*x* + 1,−*y* + 1,−*z*. Symmetry code for **2**: *a*) −*x* + 1, −*y* + 2, −*z*. Symmetry code for **3**: *a*) −*x*, −*y*, −*z*. Symmetry code for **4**: *a*) −*x*, −*y*, −*z*. Symmetry code for **5**: *a*) −*x*, −*y* + 1, −*z* + 1.

is formed in coordination complexes of $[Cu_3(dcadpz)_2(Hpz)_2(ClO_4)_2](ClO_4)_2\cdot H_2O$,[6a] *catena*-$[Cu_2\{Cu(dcadpz)_2\}(Hpz)_2(PhSO_3)_2](PhSO_3)_2$, $[Ni_2\{Cu(dcadpz)_2\}(MeOH)_2(H_2O)_4](NO_3)_4$, $[Co_2\{Cu(dcadpz)_2\}(NO_3)_2(EtOH)_2](NO_3)_2$, $[Mn_2\{Cu(dcadpz)_2\}(NO_3)_4(MeCN)_2]$,[6b] and **1**−**5**. Furthermore, when the free Hdcadpz ligand reacted with Cu(II) or Ni(II) nitrate in a 1:2 molar ratio, two mononuclear precursors of **1** and **2** were formed (Schemes 2 and 3). When **1** reacted directly with Co(II) or Ni(II) salts in common solvents, insoluble precipitates immediately appeared. In the synthesis of **3** and **4**, we first carried out the reaction of a Co(II) or Ni(II) salt with the 2,6-pdm ligand in a 1:1 molar ratio to synthesize the "$[M(pdm)]^{2+}$" (M = Co(II) and Ni(II), then precursor **1** reacted with the resulted "M(pdm)" in a 1:2 molar ratio, leading to the formation of crystals of desirable trinuclear complexes **3** and **4**. **5** can be obtained from the reaction of precursor **2** with nickel(II) nitrate in a 1:2 molar ratio by the use of DMF as a suitable solvent.

Crystal Structures. Structures of Hdcadpz and $[H_2dcadpz]^+[ClO_4]^-$. There are two unique neutral Hdcadpz molecules in the asymmetric unit of **Hdcadpz**, as shown in Figure 1. Both Hdcadpz molecules are almost coplanar with dihedral angles of 7.1° and 10.5° between the two halves. Compared with the deprotonated $dcadpz^-$ motif in the reported $[Cu_3(dcadpz)_2(Hpz)_2(ClO_4)_2](ClO_4)_2\cdot H_2O$,[6a] the position of the C═N double bond was isomerized to form a conjugating structure. The N2−C5 and N9−C12 bond distances of 1.309(3) and 1.306(3) Å are significantly shorter than the N2−C4 and N9−C13 bond distances of 1.370(3) and 1.375(3) Å, characteristic of double bonds (Scheme 1), The two C═NH groups in deprotonated $dcadpz^-$ unit are, therefore, changed from equivalent to inequivalent (the C−N bond distances for the C═NH groups are 1.262(3) and 1.272(3) Å, and the C−N bond distances for the $C-NH_2$ groups are 1.302(3) and 1.306(3) Å). Within each neutral Hdcadpz molecule, a hydrogen bond was formed between the intramolecular NH_2 and NH groups (N⋯N = 2.648(3) and 2.644(3) Å; ∠N−H⋯N = 129(2)° and 130(2)°). Moreover, adjacent Hdcadpz units are interlinked into a 3D supramolecular architecture (Figure S2) via the rich intermolecular hydrogen bonds among the pyrazoyl groups and NH_2 and NH groups (N⋯N = 2.995(3)−3.329(3) Å; ∠N−H⋯N = 149(2)−160(2)°).

In the crystal structure of $[H_2dcadpz]^+[ClO_4]^-$ (Figure 2a), the asymmetric unit contains one-half of a protonated Hdcadpz molecule and a disordered ClO_4^- anion with an occupancy of 0.5. Similar to that in Hdcadpz, the position of the C═N double bond was also isomerized to form a conjugating structure (Scheme 1). However, the C═NH and $C-NH_2$ groups turn out to be undistinguishable due to the protonation of the C═NH group (into a $C{=}NH_2^+$ group). Interestingly, the protonated Hdcadpz molecule is noncoplanar with a dihedral angle of 50.7° between the two halves. Adjacent $[H_2dcadpz]^+$ units are interlinked into 1D helical chains along the *b* axis (Figure 2b) via the intermolecular self-complementary hydrogen bonds between the pyrazoyl N groups and NH_2 groups (N⋯N = 3.013(4) Å; ∠N−H⋯N = 147(4)°). The perchlorate anions are located between these helical chains and form a 3D supramolecular architecture (Figure S3) via rich interchain N−H⋯O and C−H⋯O hydrogen bonds (N⋯O = 2.95(1)−3.10(1), C⋯O = 3.192−3.455 Å; ∠N−H⋯O = 146(4)−149(4)°, ∠C−H⋯O = 127.3−153.9°).

Scheme 1. Schematic Showing the Separation Process of the Hdcadpz Ligand

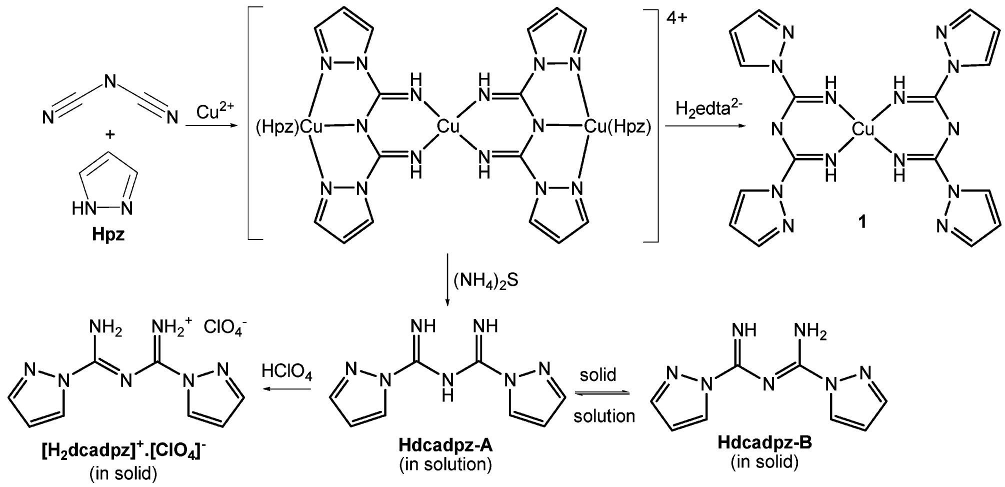

Scheme 2. Schematic Showing the Synthesis of **3** and **4** from the Metalloligand $[Cu(dcadpz)_2]$ Precursor

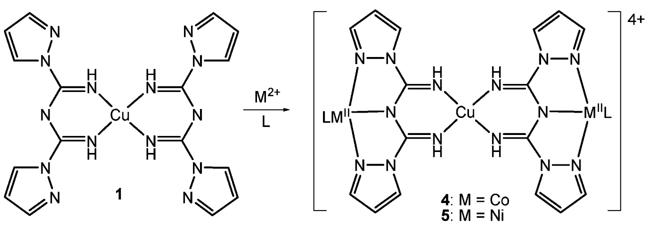

Structures of $[Cu(dcadpz)_2]$ (1) and $[Ni(dcadpz)_2]\cdot 2/3DMF$ (2). **1** crystallizes in tetragonal $P4_2/n$ space group with an asymmetric unit consisting of half a formula unit (Figure 3). The copper atom is located on the inversion center and is coordinated in a slightly disordered square planar environment by four nitrogen atoms (Cu−N = 1.926(3) and 1.936(3) Å; ∠cis-N−Cu−N = 87.1(1)° and 92.9(1)°), forming two six-membered metallocycles. The N(1)−C(1) and N(3)−C(2) distances of 1.293(5) and 1.291(4) Å and C(1)−N(2) and C(2)−N(2) of 1.328(4) and 1.331(4) Å, respectively, indicate a strongly delocalized π-bonding system, similar to those found in related compounds of $[Cu(dcadMeOH)_2]$ (dcadMeOH = bis(methoxycarbimido)aminato)[11e] and $[Cu_3(dcadpz)_2(Hpz)_2(ClO_4)_2](ClO_4)_2\cdot H_2O$.[6a] The $\pi-\pi$ stacking interaction exists between different units with the face-to-face distance of 3.213−3.466 Å, which extends the neutral mononuclear complex of **1** into 1D supramolecular columns along the *c* axis (Figure 3b,c).

2 crystallizes in monoclinic $P2_1/n$ space group and the asymmetric unit consists of one and a half formula units, and therefore, there are two crystallographically unique (but chemically similar) metal environments (Figure 4a,b). The Ni1 atom is located on the inversion center and is coordinated in an almost ideal square planar environment by four nitrogen atoms (Ni1−N = 1.857(4) and 1.853(4) Å; ∠cis-N−Ni1−N = 89.7(2)° and 90.3(2)°), similar to that in **1**. The N(1)−C(1) and N(3)−C(2) distances of 1.300(5) and 1.304(5) Å and C(1)−N(2) and C(2)−N(2) of 1.318(5) and 1.320(5) Å, respectively, indicate a strongly delocalizated π-bonding system, similar to those found in **1**. The Ni2 atom is located on a general position, and its coordination geometry is similar to Ni1 (Ni2−N = 1.850(3)−1.872(3) Å; ∠cis-N−Ni2−N = 89.2(2)−91.8(2)°). Different from that in **1**, each Ni1 motif stacks in the center with a pair of Ni2 motifs in a face-to-face fashion into a stacking $([Ni(dcadpz)_2])_3$ aggregate with distances of 3.314(3) and 3.566(3) Å and dihedral angles of 0.8° and 1.3°. Furthermore, the $\pi-\pi$-stacked $([Ni(dcadpz)_2])_3$ aggregates are further extended by the edge-to-face interaction (Figure 4c) into a 3D supramolecular architecture, different from that found in **1**.

Structures of $[\{M(pdm)\}_2\{Cu(dcadpz)_2\}](NO_3)_4$ ($M = Co^{2+}$, 3; Ni^{2+}, 4). **3** and **4** are isostructural linear trinuclear MCuM ($M = Co^{2+}$ and Ni^{2+}) complexes, as illustrated in Figure 5a, b. The crystallographically asymmetric unit consists of half of a Cu(II) atom, which is located on an inversion center, one Co(II) or Ni(II) atom, which is located on a general position, one $dcadpz^-$, one pdm, and two NO_3^- anions. The central Cu1 atom is ligated in a slightly distorted square planar geometry by four nitrogen atoms from two dcadpz ligands with Cu1−N bond lengths of 1.952(3)−1.963(3) Å for **3** and 1.950(3)−1.962(3) Å for **4**, respectively, similar to those found in $[Cu_3(dcadpz)_2(Hpz)_2(ClO_4)_2](ClO_4)_2\cdot H_2O$[6a] but longer than those in **1**. Each of the terminal Co or Ni atoms is coordinated in a greatly distorted MN_4O_2 octahedral geometry (∠cis-N/O−M−N/O = 74.76(9)−119.64(9)°, ∠trans-N/O−M−N/O = 144.3(1)−165.2(1)° for **3**; ∠cis-N/O−M−N/O = 78.0(1)−105.7(1)°, ∠trans-N/O−M−N/O = 156.1(1)−174.9(1)° for **4**) to three nitrogen atoms from a dcadpz ligand and one nitrogen atom and two oxygen atoms from a pdm ligand with M−N and M−O bond lengths of 2.070(3)−2.119(3) and 2.175(2)−2.177(2) Å for **3** and 1.992(3)−2.054(4) and 2.107(3)−2.134(3) Å for **4**, respectively. The intra-trinuclear Cu1···Co1 and Cu1···Ni1 distances are 5.411 and 5.335 Å, whereas the shortest inter-trinuclear Co···Co and Ni···Ni distance are 7.482 and 7.731 Å for **3** and **4**, respectively. Along the *a* axis, each trinuclear MCuM unit further connects with adjacent units via both $\pi-\pi$ stacking between the intertrinuclear pyrazoyl groups and C−H(pyrazoyl)···O(pdm) hydrogen-bonding interactions into 1D stair-type supramolecular chains (Figure S4), which are further extended into 2D layers (Figure 5c) via offset $\pi-\pi$ stacking interaction between the interchain pdm groups. Finally, a 3D supramolecular architecture is resulted from

Scheme 3. Schematic Showing the Stepwise Synthesis of **2** and **5**

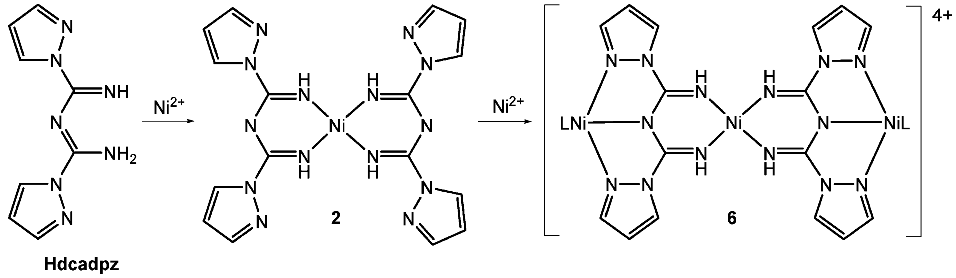

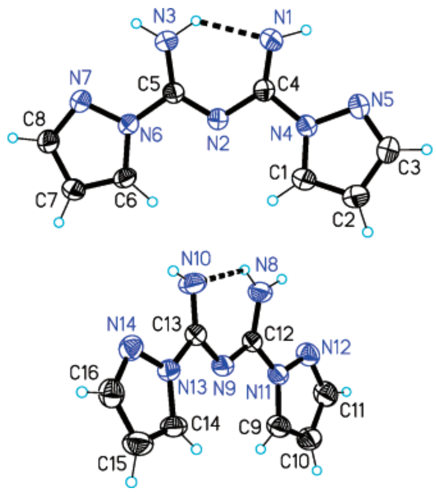

Figure 1. Molecular structure of the Hdcadpz ligand; 50% thermal ellipsoids are shown.

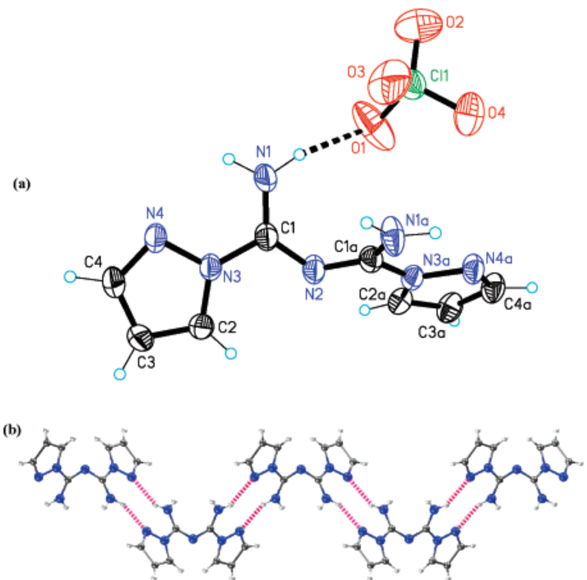

Figure 2. Molecular structure of $[H_2dcadpz]^+[ClO_4]^-$ (a); 50% thermal ellipsoids are shown. (b) The 1D helical chain along the *b* axis.

the O−H(pdm)···O(NO_3^-) hydrogen-bonding interactions between the nitrate anions and the imino groups.

Structure of [{Ni(MeOH)(H_2O)$_2$}$_2${Ni(dcadpz)$_2$}](NO_3)$_4$ (5). **5** is a symmetrical linear homotrinuclear nickel(II) complex. The crystallographically asymmetric unit consists of 1.5 Ni(II) atoms, one dcadpz, one MeOH and two aqua ligands as well as two NO_3^- anions in the crystal structure (Figure 6). The central Ni1 is located on an inversion center and coordinated in a slightly distorted square planar geometry

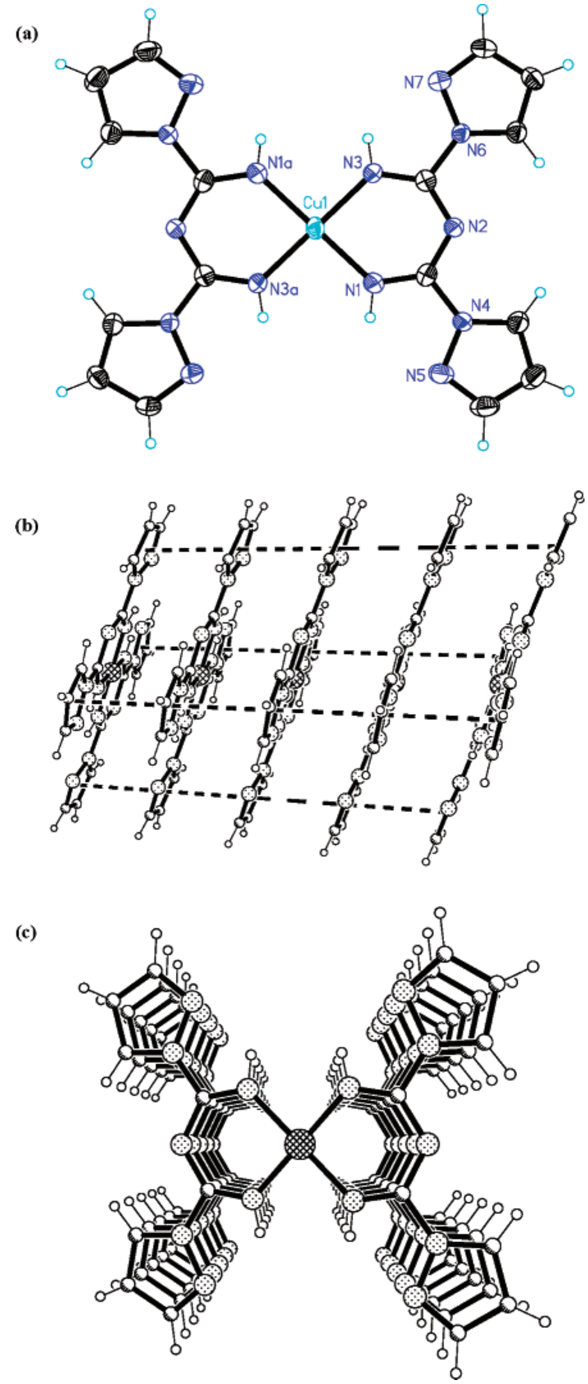

Figure 3. Molecular structure of **1** (a); 50% thermal ellipsoids are shown. Side (b) and top (c) views of 1D supramolecular column in **1**.

to four nitrogen atoms from two dcadpz$^-$ ligands with Ni1−N bond lengths of 1.883(3) and 1.877(3) Å and ∠cis-

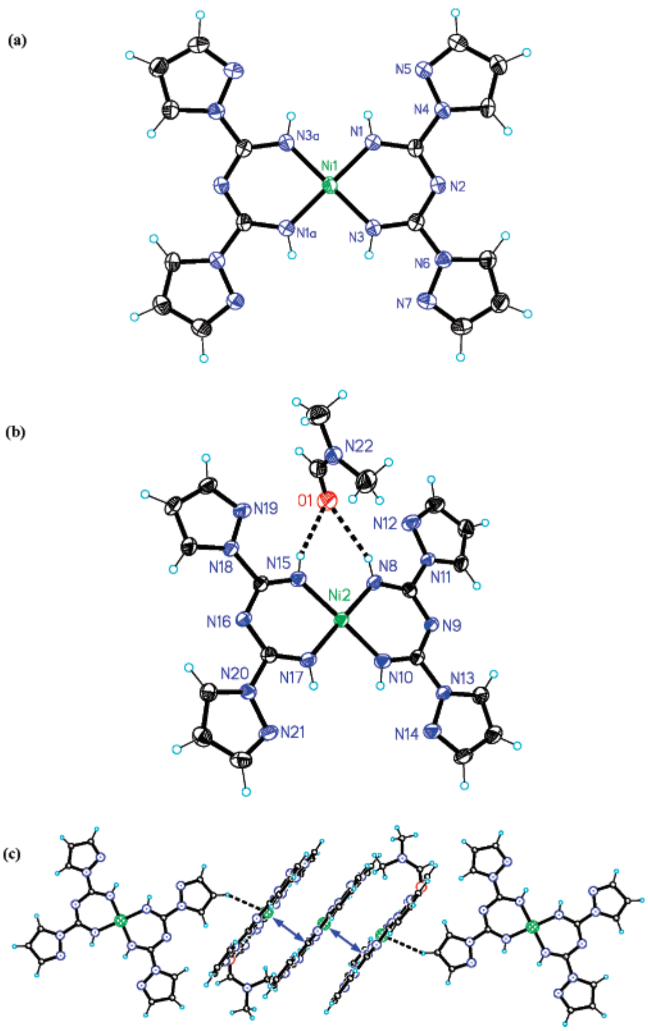

Figure 4. Molecular structure of **2** (a and b); 50% thermal ellipsoids are shown. (c) The $\pi-\pi$ stacking and the edge-to-face interactions in **2**.

N−Ni−N = 89.1(1)−90.9(1)°, which are comparable with those in **2**. Each of the terminal Ni2 atoms is coordinated in a greatly distorted octahedral geometry with three nitrogen atoms from the dcadpz$^-$ ligand with Ni2−N bond lengths of 2.015(3)−2.058(3) Å, and two aqua ligands and one MeOH ligand with Ni2−O bond lengths of 2.034(3)−2.094(3) Å and N/O−Ni2−N/O bond lengths of 2.034(3)−2.094(3) Å and ∠cis-N/O−M−N/O bond angles of 78.1(1)−102.6(1)°, ∠trans-N/O−M−N/O bond angles of 156.6(1)−177.8(1)°. The intra-trinuclear Ni1···Ni2 distance is 5.265 Å, whereas the intra-trinuclear Ni2···Ni2a distance and the shortest inter-trinuclear Ni2···Ni2a distance are 10.530 and 6.890 Å, respectively. Each trinuclear Ni_3 unit further connects with adjacent Ni_3 units via N_{dcadpz}−H···O, $O_{pdm,water}$−H···O and C−H···O hydrogen-bonded interactions, resulting in a 3D supramolecular architecture (Figure S5). Notably, the reported linear trinuclear nickel(II) complexes are those trinuclear structures with all octahedral geometry about the nickel centers,[13] and those with mixed square-pyramidal/square-planar/square-pyramidal and square-pyramidal/octahedral/square-pyramidal geometry.[14]

Magnetic Properties. The dc magnetic properties of **3** in the form of $\chi_M T$ vs T and M vs H plots (χ_M is the magnetic

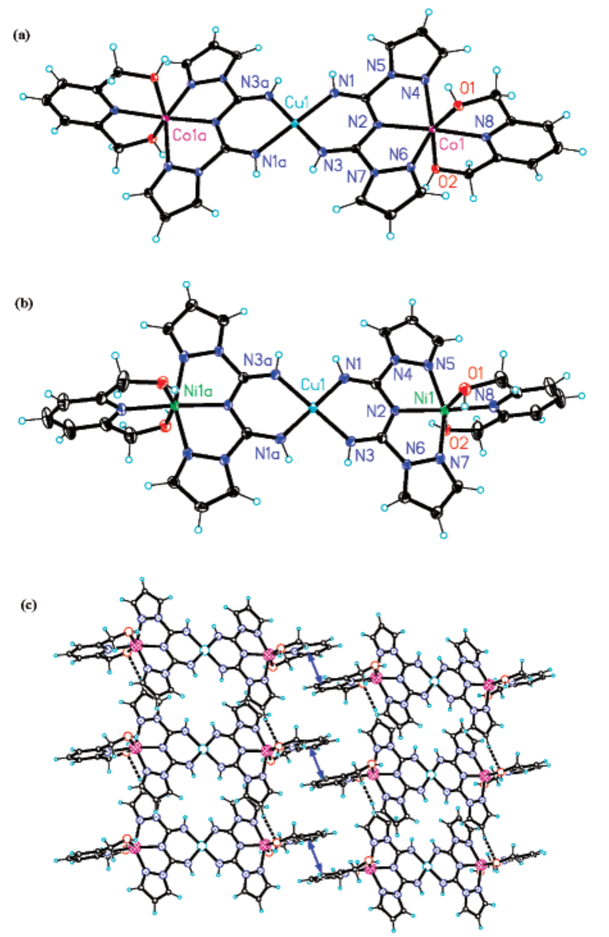

Figure 5. Coordination environments of the metal ions in **3** (a) and **4** (b); 50% thermal ellipsoids are shown. (c) The 2D supramolecular layer in **3**.

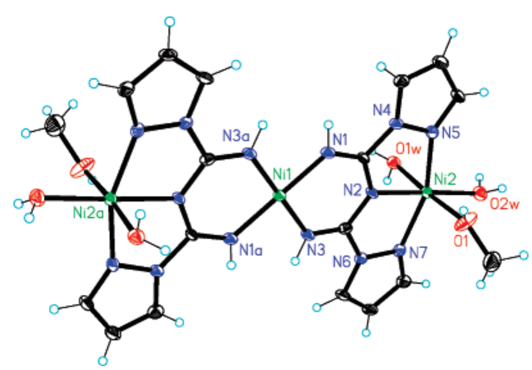

Figure 6. Coordination environments of the metal ions in **5**; 50% thermal ellipsoids are shown.

susceptibility per trinuclear unit) are shown in Figure 7. The 50−300 K temperature dependences of the magnetic susceptibility was well fit by the Curie−Weiss expression, $\chi = C/(T-\theta) + \chi_0$, with $C = 6.18$ cm^3 mol^{-1} K, $\theta = -4.83$ K,

(13) (a) Cano, J.; De Munno, G.; Lloret, F.; Julve, M. *Inorg. Chem.* **2000**, *39*, 1611. (b) Xu, Z.; Thompson, L. K.; Milway, V. A.; Zhao, L.; Kelly, T.; Miller, D. O. *Inorg. Chem.* **2003**, *42*, 2950. (c) Heinicke, J.; Peulecke, N.; Karaghiosoff, K.; Mayer, P. *Inorg. Chem.* **2005**, *44*, 2137. (d) Beissel, T.; Birkelbach, F.; Bill, E.; Glaser, T.; Kesting, F.; Krebs, C.; Weyhermuller, T.; Wieghardt, K.; Butzlaff, C.; Trautwein, A. X. *J. Am. Chem. Soc.* **1996**, *118*, 12376.

(14) (a) Clerac, R.; Cotton, F. A.; Dunbar, K. R.; Murillo, C. A.; Pascual, I.; Wang, X. *Inorg. Chem.* **1999**, *38*, 2655. (b) Bu, X.-H.; Du, M.; Zhang, L.; Liao, D.-Z.; Tang, J.-K.; Zhang, R.-H.; Shionoya, M. *J. Chem. Soc., Dalton Trans.* **2001**, 593.

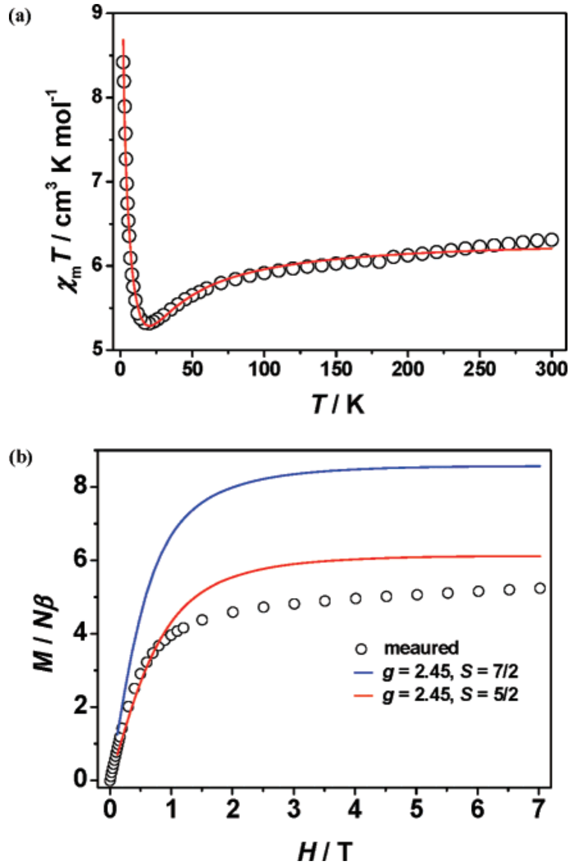

Figure 7. (a) Plot of the $\chi_M T$ vs T. Solid lines represent the best fit with the parameters given in the text for **3**. (b) The field dependence of the magnetization measured at 2 K (scattered open circles) for **3**. The Solid lines represent the theoretical curve per $CuCo_2$ unit calculated with the Brillouin functions with different spins.

and $\chi_o = 2.6 \times 10^{-4}$ cm^3 mol^{-1} (fixed) (Figure S6a). The C value coresponds to $g = 2.45$. The $\chi_M T$ values at room temperature are 6.31 cm^3 mol^{-1} K, which are greatly larger than that expected for the sum of the spin-only values of a square-planar Cu^{II} ion ($S_{Cu} = 1/2$, $\chi_M T = 0.375$ cm^3 mol^{-1} K with $g = 2.0$) and two octahedral high-spin Co^{II} ions ($S_{Co} = 3/2$, $\chi_M T = 3.75$ cm^3 mol^{-1} K with $g = 2.0$) in magnetic isolation. On cooling, $\chi_M T$ decreases, and it attains a minimum at 20 K and increase smoothly upon cooling further, which is typical of ferrimagnetic linear trinuclear M(II)−M(II)−M(II) cluster compounds which exhibits a characteristic minimum.[15] From the structural analysis, **3** is considered to consist of well-separated trinuclear cluster units. The temperature dependence of $\chi_M T$ was analyzed by an isotropic isolated three-spin model[1a] ($H = -2J(S_{Co1}\cdot S_{Cu1} + S_{Cu1}\cdot S_{Co1'})$) within MAGMUN4.1.[16] The best-fit parameters were $J = -5.27$ cm^{-1}, $zJ' = 0.056$ cm^{-1}, $g_{av} = 2.48$, $R = 1.6 \times 10^{-4}$ ($R = [\sum(\chi_{obs} - \chi_{calcd})^2/\sum\chi_{obs}{}^2]^{1/2}$). These fitting results reveal that the $Cu(dcadpz)_2$ is antiferromagnetically coupled with both the terminal Co(II) ions, and therefore, each Co−Cu−Co unit exhibits ferrimagnetic behavior and

(15) Tercero, J.; Diaz, C.; Ribas, J.; Maestro, M.; Mahía, J.; Stoeckli-Evans, H. *Inorg. Chem.* **2003**, *42*, 3366.
(16) *MAGMUN4.1* is freely available through http://www.ucs.mun.ca/∼lthomp/magmun.html. The program may be used for scientific purposes only. Reference to it should be quoted appropriately.

Scheme 4. Schemes of the Spin Topology Assuming Intramolecular Magnetic Coupling in the Trinuclear Systems of **3**, **4**, and **5**

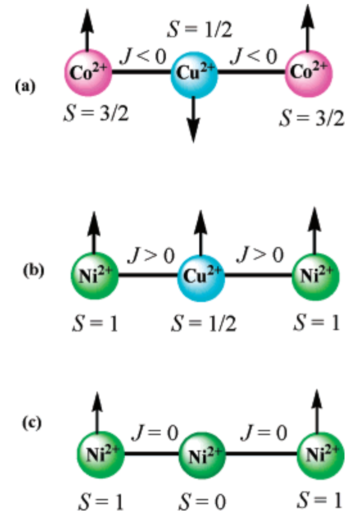

has a ground spin multiplicity of 5/2, which is supported by the field dependence of the magnetization. At 2 K, the molar magnetizations per Co−Cu−Co unit in the field range of 0−7 T are shown in Figure 7b together with the Brillouin magnetization curves for the uncoupled Co−Cu−Co cluster and the coupled states. The experimental curve gradually approaches the theoretical curve (solid line in Figure 7b) of M/H for the $S = 5/2$ state, in agreement with the ground state calculated from the vector coupling scheme (Scheme 4a) for the Co−Cu−Co cluster and consistent with the analysis of the variable-temperature magnetic data.

For **4**, the $\chi_M T$ value at room temperature is 2.86 cm^3 mol^{-1} K (Figure 8a), which is significantly larger than that expected for the sum of the spin-only values of a square-planar Cu^{II} ion ($S_{Cu} = 1/2$, $\chi_M T = 0.375$ cm^3 mol^{-1} K with $g = 2.0$) and two octahedral high-spin Ni^{II} ions ($S_{Ni} = 1$, $\chi_M T = 2.0$ cm^3 mol^{-1} K with $g = 2.0$) in magnetic isolation due to the orbital contribution of Ni(II) ions. On cooling, the $\chi_M T$ product increases monotonically and reaches 3.07 cm^3 mol^{-1} K at 9 K, which is typical of ferromagnetic NiCuNi trinuclear cluster compounds (Scheme 4b).[6b] Below 9 K, the $\chi_M T$ value decreases rapidly caused by the zero-field splitting with $\chi_M T$ value of 2.2 cm^3 mol^{-1} K at 2 K. The 50−300 K temperature dependences of the magnetic susceptibility was well fit by the Curie−Weiss expression, $\chi = C/(T - \theta) + \chi_0$, with $C = 2.77$ cm^3 mol^{-1} K, $\theta = 1.99$ K, and $\chi_o = 2.6 \times 10^{-4}$ cm^3 mol^{-1} (fixed) (Figure S6b). The C value coressponds to $g = 2.16$. To fit the experimental data, we used the theroetical expression of the magnetic susceptibility deduced from the spin-Hamiltonian equation[17] $H = -J(S_{Ni1}\cdot S_{Cu} + S_{Cu}\cdot S_{Ni1'}) + D[S_z^2 - 1/3S(S+1)] + \beta[g_{Ni}(S_{Ni1} + S_{Ni1'}) + g_{Cu}S_{Cu}]H$, the parallel and perpendicular magnetic susceptibilities are then

(17) (a) Kahn, O. *Struct. Bonding* **1987**, *68*, 89. (b) Pei, Y.; Journaux, Y.; Kahn, O. *Inorg. Chem.* **1988**, *27*, 399. (c) Vecente, R.; Escuer, A.; Ribas, J. *Polyhedron* **1992**, *11*, 857. (d) Ribas, J.; Diaz, C.; Costa, R.; Journaux, Y.; Mathoniere, C.; Kahn, O.; Gleizes, A. *Inorg. Chem.* **1990**, *29*, 2042. (e) Miao, M.-M.; Cheng, P.; Liao, D.-Z.; Jiang, Z.-H.; Wang, G.-L. *Transition Met. Chem.* **1997**, *22*, 19.

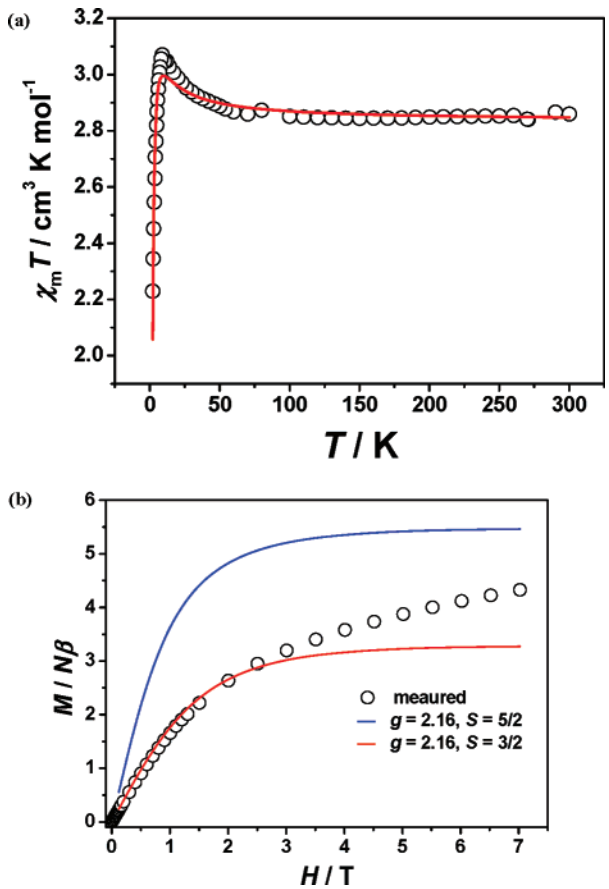

Figure 8. (a) Plot of $\chi_M T$ vs T. Solid lines represent the best fit with the parameters given in the text for **4**. (b) The field dependence of the magnetization measured at 2 K (scattered open circles) for **4**. The Solid lines represent the theoretical curve per $CuNi_2$ unit calculated with the Brillouin functions with different spins.

$$\chi_{\parallel} = (N\beta^2/4kT)\{g_{3/2,2}{}^2[9\exp(-D/kT) + \exp(D/kT)] + g_{1/2,1}{}^2\exp(J/2kT) + g_{1/2,0}{}^2\exp(3J/2kT) + 10g_{3/2,1}{}^2 \times \exp(2J/kT) + 35g_{5/2,2}{}^2\exp(5J/2kT)\}/\{\exp(-D/kT) + \exp(D/kT) + \exp(J/2kT) + \exp(3J/2kT) + 2\exp(2J/kT) + 3\exp(5J/2kT)\}$$

$$\chi_{\perp} = (N\beta^2/4kT)\{g_{3/2,2}{}^2[-(3kT/D)\exp(-D/kT) + (4 + 3kT/D)\exp(D/kT)] + g_{1/2,1}{}^2\exp(J/2kT) + g_{1/2,0}{}^2\exp(3J/2kT) + 10g_{3/2,1}{}^2\exp(2J/kT) + 35g_{5/2,2}{}^2\exp(5J/2kT)\}/\{\exp(-D/kT) + \exp(D/kT) + \exp(J/2kT) + \exp(3J/2kT) + 2\exp(2J/kT) + 3\exp(5J/2kT)\}$$

$$g_{3/2,2} = (6g_{Ni} - g_{Cu})/5, \quad g_{1/2,1} = (4g_{Ni} - g_{Cu})/3, \quad g_{1/2,0} = g_{Cu}, \quad g_{3/2,1} = (2g_{Ni} + g_{Cu})/3, \quad g_{5/2,2} = (4g_{Ni} + g_{Cu})/5$$

The least-square fitting of the experimental data leads to two equally satisfying solutions, according to whether D is positive or negative. The parameters of these two solutions are $J = 2.50$ cm^{-1}, $g_{Ni} = 2.19$, $g_{Cu} = 2.12$, $D = \pm 10.01$ cm^{-1}, $R = 1.81 \times 10^{-3}$ ($R = [\sum(\chi_{obs}T - \chi_{calcd}T)^2/\sum(\chi_{obs}T)^2]^{1/2}$). These fitting results reveal that the $Cu(dcadpz)_2$ is ferromagnetically coupled with both the terminal Ni(II) ions, and therefore, each Ni−Cu−Ni unit has a ground spin multiplicity of 5/2. At 2 K, the molar magnetizations per Ni−Cu−Ni unit in the field range of 0−7 T are shown in Figure 8b together with the Brillouin magnetization curves for the uncoupled Ni−Cu−Ni cluster and the coupled states (Scheme 4b). The experimental curve gradually approaches the theoretical curve (solid line in Figure 7b) of M/H for the $S = 5/2$ state ($g = 2.16$) but is far from the theoretical curve (solid line in Figure 8b) of M/H for the $S = 3/2$ state ($g = 2.16$).

For **5**, the central square-planar Ni^{II} ion is diamagnetic ($S_{Ni} = 0$, $\chi_M T = 0$), the $\chi_M T$ values at room temperature is 2.47 cm^3 mol^{-1} K, which is larger than that expected for the sum of the spin-only values of two magnetically isolated octahedral high-spin Ni^{II} ions ($S_{Ni} = 1$, $g = 2.0$, $\chi_M T = 2.00$ cm^3 mol^{-1} K, Scheme 4c) due to the orbital contribution of Ni(II) ions. On cooling, $\chi_M T$ shows a slight decrease between 300 and 17.0 K. The 50−300 K temperature dependences of the magnetic susceptibility, was well fit by the Curie−Weiss expression, $\chi = C/(T - \theta) + \chi_0$, with $C = 2.41$ cm^3 mol^{-1} K, $\theta = -2.23$ K, and $\chi_o = 2.0 \times 10^{-4}$ cm^3 mol^{-1} (Figure S6c). The C value corresponds to $g = 2.19$. Below 17 K, the $\chi_M T$ value decreases rapidly caused by the zero-field splitting.

To take account of the effect of zero-field splitting, we deduced the average magnetic susceptibility from the parallel and perpendicular magnetic susceptibility, $\chi = (4N\beta^2 g_z{}^2/3kT)\{[4\exp(-D/kT)]/[1 + 2\exp(-D/kT)]\} + (8N\beta^2 g_x{}^2/3D)\{[1 - \exp(-D/kT)]/[1 + 2\exp(-D/kT)]\} + \mathrm{TIP}$.

The least-square fitting of the experimental data leads to $D = 5.91$ cm^{-1} and $g_x = 2.02$, $g_z = 2.47$ with TIP $= 2.0 \times 10^{-4}$ cm^3 mol^{-1} (Figure 9a). The average g is 2.19 calculated from $g^2 = (g_x{}^2 + g_y{}^2 + g_z{}^2)/3$. At 2 K, the molar magnetizations of **5** (per Ni_3 unit) in the field range of 0−7 T are shown in Figure 9b. The experimental curve gradually approaches the theoretical curve (bold line) of M/H for the $S = 2$ state ($g = 2.19$).

It is interesting to note that the magnetic orbital of Cu1 in the neutral $Cu(dcadpz)_2$ metalloligand is regarded as $d_{x^2-y^2}$ which directs toward the four basal N atoms from two $dcadpz^-$ ligands, similar to that found in the reported pioneering building blocks, for example, $[Cu(opba)]^{2-}$ (opba =*o*-phenylenebis(oxamato)), $[Cu(bpca)_2]$ and $[Fe(bpca)(CN)_3]^-$ (Hbpca = bis(2-pyridylcarbonyl)amine).[2a,18,19] The magnetic orbitals of the terminal Co(II) or Ni(II) atom, are mainly d_{z^2}, $d_{x^2-y^2}$, lies in the N_2O_2 plane perpendicular to the $Cu(dcadpz)_2$ plane. The orientations of the magnetic orbits in linear trinuclear MCuM (M = Cu^{2+}, Mn^{2+}, Co^{2+}, and Ni^{2+}) species have been summarized by us and Igashira-Kamiyama et al. [6a,b] In **4** (Ni−Cu−Ni), the ferromagnetic coupling resulting from the orthogonality of the symmetric magnetic orbitals ($d_{x^2-y^2}$ and d_{z^2}) of the terminal Ni(II) ions and

(18) (a) Kajiwara, T.; Kamiyama, A.; Ito, T. *Chem. Commun.* **2002**, 1256. (b) Kamiyama, A.; Noguchi, T.; Kajiwara, T.; Ito, T. *CrystEngComm* **2003**, *42*, 231. (c) Glaser, T.; Theil, H.; Liratzis, I.; Weyhermu1ller, T.; Bill, E. *Inorg. Chem.* **2006**, *45*, 4889.

(19) (a) Wen, H.-R.; Wang, C.-F.; Zuo, J.-L.; Song, Y.; Zeng, X.-R.; You, X.-Z. *Inorg. Chem.* **2006**, *45*, 582. (b) Liu, W.; Wang, C.-F.; Li, Y.-Z.; Zuo, J.-L.; You, X.-Z. *Inorg. Chem.* **2006**, *45*, 10058.

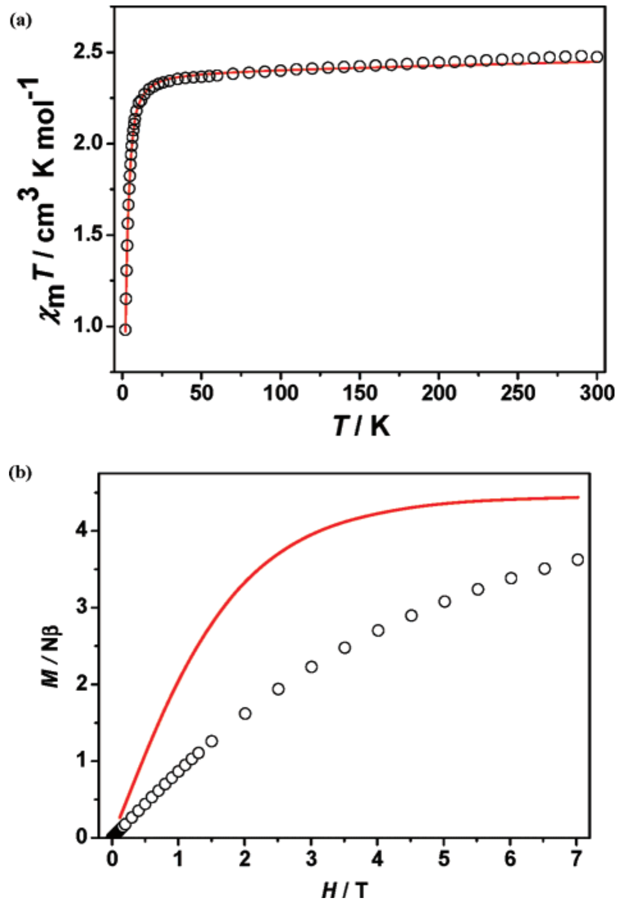

Figure 9. (a) Plot of $\chi_M T$ vs T for **5**. (b) The field dependence of the magnetization measured at 2 K for **5**. The Solid line represent the theoretical curve per Ni_3 unit calculated with the Brillouin function with $g = 2.19$ and $S = 2$.

antisymmetric magnetic orbital of the central Cu(II) ion, whereas in **3** (Co−Cu−Co), each terminal Co(II) ion has both dσ spins in e_g orbitals and dπ spins in t_{2g} orbitals. Therefore, the total magnetic interaction depends on the sum of two opposite interactions, the antiferromagnetic magnetic interaction between $e_g(Cu_{central})$ and $t_{2g}(Co_{terminal})$ through space type, and the ferromagnetic interaction between $e_g(Cu_{central})$ and $e_g(Co_{terminal})$. The experimental data of **3** show that the antiferromagnetic interaction ($e_g(Cu_{central})-t_{2g}(Co_{terminal})$) slightly dominates over the ferromagnetic interaction ($e_g(Cu)-t_{2g}(Co)$), leading to an overall ferrimagnetic interaction occurred in **3**, which is different from that observed for $[Co_2\{Cu(dcadpz)_2\}(NO_3)_2(EtOH)_2](NO_3)_2$.[6b] The difference in magnetic interactions may result from the significant distortion in the coordination geometry around Co(II) due to the introduction of tridentate pdm ligand.

Conclusions

In this study, we have isolated a neutral pentadentate ligand, di(pyrazolecarbimido)amine (Hdcadpz), from our previously synthesized linear trinuclear $[Cu_3(dcadpz)_2(Hpz)_2(ClO_4)_2](ClO_4)_2\cdot H_2O$.[6a] Characterization of X-ray crystallography, NMR, MS, EA, and IR technique reveals that it can exist in four forms of Hdcadpz-A (in solution), Hdcadpz-B (solid), $[H_2dcadpz]^+$ (solid), and $[dcadpz]^-$ (coordinated) under different conditions. Two mononuclear $M(dcadpz)_2$ ($M = Cu^{II}$ and Ni^{II}) precursors can be obtained by reacting copper(II) or nickel(II) nitrate with Hdcadpz in 1:2 molar ratio. Two mononuclear precursors can be rationally combined with Co(II) or Ni(II) ions to obtain three homo- and heterotrinuclear clusters exhibiting ferromagnetic, ferrimagnetic, and paramagnetic behaviors, respectively, which provides a new route to magnetic homo- and heterotrinuclear clusters.

Acknowledgment. This work was supported by the NSFC (No. 20525102), the National Basic Research Program of China (2007CB815305) and SRFDP (20060558081).

Supporting Information Available: X-ray crystallographic files of Hdcadpz, $[H_2dcadpz]^+[ClO_4]^-$, and **1**−**5** (CIF), UV−vis spectra, four structural plots, and additional plots for magnetic studies. This material is available free of charge via the Internet at http://pubs.acs.org.

IC070343Z